



## Hydrothermal synthesis of perovskite strontium doped lanthanum chromite fine powders and its sintering

J.C. Rendón-Angeles<sup>a,b,\*</sup>, K. Yanagisawa<sup>b</sup>, Z. Matamoros-Veloza<sup>c</sup>, M.I. Pech-Canul<sup>a</sup>, J. Mendez-Nonell<sup>a</sup>, S. Diaz-de la Torre<sup>d</sup>

<sup>a</sup> Research Institute for Advanced Studies of the NPI, Campus-Salttillo, Ramos Arizpe 25900, Coah., Mexico

<sup>b</sup> Research Laboratory of Hydrothermal Chemistry, Kochi University, Kochi 780-8520, Japan

<sup>c</sup> Saltillo Institute of Technology, Dep. Metal-Mecánica, Saltillo 25820, Coah., Mexico

<sup>d</sup> Research Institute for Technology Innovation, CIITEC-IPN, Azcapotzalco 02250, Mexico

### ARTICLE INFO

#### Article history:

Received 13 October 2009

Accepted 19 May 2010

Available online 2 June 2010

#### Keywords:

Lanthanum chromite

Coprecipitation

Hydrothermal synthesis

Sintering

Electrical conductivity

### ABSTRACT

Sr doped lanthanum chromite powders with two different compositions,  $\text{La}_{0.9}\text{Sr}_{0.1}\text{CrO}_3$  and  $\text{La}_{0.8}\text{Sr}_{0.2}\text{CrO}_3$ , were prepared from precursor lanthanum chromite gels obtained by the coprecipitation method, followed by hydrothermal treatments at temperatures from 400 to 450 °C, for various reaction times varying from 0.5 to 2 h. The reaction products were characterized by XRD, SEM and TEM techniques. The powder was cold isostatically pressed at 200 MPa, and then sintered in air at 1500 °C for several intervals (1–20 h). Relative density measurements were conducted by helium pycnometry and the microstructure was revealed by SEM after thermal etching. The X-ray diffraction patterns of the powders corresponding to  $\text{La}_{0.9}\text{Sr}_{0.1}\text{CrO}_3$  and  $\text{La}_{0.8}\text{Sr}_{0.2}\text{CrO}_3$  nominal compositions obtained at 400 and 425 °C for 1 h, respectively, were indexed with that of the orthorhombic single  $\text{LaCrO}_3$  phase. SEM and TEM micrographs showed that the particles had irregular peanut-like morphology, and the average particle size was 300 nm. Furthermore, the maximum relative density of the  $\text{La}_{0.8}\text{Sr}_{0.2}\text{CrO}_3$  sample obtained by the heat treatment in air at 1500 °C for 20 h was 97% of the theoretical density and the average grain size of the sintered pellet was of 5 μm. The electric conductivity and activation energy determined for this pellet were  $14477.3 \text{ S m}^{-1}$  and 0.13 eV, respectively.

© 2010 Elsevier B.V. All rights reserved.

### 1. Introduction

Lanthanum chromite powders have been widely used as interconnector in solid oxide fuel cells (SOFCs) [1]. However, the  $\text{LaCrO}_3$  pure phase has a high melting point (2590 °C) and it is difficult to obtain fully densified  $\text{LaCrO}_3$  monoliths, which is the main problem in manufacturing SOFC separators [2]. The lanthanum chromite compounds which continuing under exhaustive investigation are the solid solutions with general chemical formula:  $\text{La}_{1-x}\text{M}_x\text{BO}_3$  where M is an alkaline earth metal such as Ca, Mg or Sr, while the metal ions that can be incorporated at the B site are Cr, Mn or Fe. These compounds exhibit a high electrical conductivity and excellent chemical stability under reducing and oxidizing atmospheres during the operation of the SOFC device [3,4]. The  $\text{La}_{1-x}\text{M}_x\text{CrO}_3$  type solid solutions have widely demonstrated to achieve high relative densities, typically above 94% of the theoretical density, by

sintering at 1600 °C even in air atmosphere [5]. Moreover, Sr doped  $\text{LaCrO}_3$  are preferred as interconnector due to its high thermal stability, in contrast with the Ca substituted  $\text{LaCrO}_3$  interconnectors, because this compound commonly exhibits a  $\text{Ca}^{2+}$  migration from the interconnector to other parts of the SOFC cell during the sintering stage. In addition, the  $\text{Ca}^{2+}$  migration inhibits the densification of Ca doped interconnectors which causes the degradation of the SOFC device during operating conditions [6].

Recently, various chemical routes have been used for processing powders of lanthanum chromite doped with strontium, namely glycine nitrate [7,8], emulsion [9], and Pechini's process [10–12], but these chemical routes involve heat treatments at temperatures in the range of 700–900 °C for a heat treatment time of 2–12 h, in order to obtain the crystalline phase. Group et al. [10] obtained various solid solutions with different contents of Sr between 0 and 20 mol% by the Pechini method. The crystalline orthorhombic  $\text{LaCrO}_3$  phase was obtained by subsequent heat treatments at 800 °C. The powders produced by this route had an average particle size of 100 nm, and a relative density over 95% was achieved by sintering the powders at 1740 °C for 1 h under reducing atmosphere. In addition, it was recently found that nanometric chemically derived Sr doped  $\text{LaCrO}_3$  powders had good sinterability even in

\* Corresponding author at: Research Institute for Advanced Studies of the NPI, Campus-Salttillo, Ramos Arizpe, 25900 Coah., Mexico.

Tel.: +52 844 438 9600x9672; fax: +52 844 438 9600x9610.

E-mail address: [jcarlos.rendon@cinvestav.edu.mx](mailto:jcarlos.rendon@cinvestav.edu.mx) (J.C. Rendón-Angeles).

air atmosphere, and relative densities over the range of 93–96% were normally achieved at temperature as low as 1600 °C [7–9,13].

The aforementioned efforts conducted to improve the sinterability of Sr doped  $\text{LaCrO}_3$  solid solutions account for several characteristics of the raw powder, such as chemical compositional homogeneity, high purity, controlled particle morphology, and nanometric particle size. Moreover, a wide variety of raw oxide powders have been prepared by means of the hydrothermal technique. The powders prepared by this technique have particular morphological and compositional features which are required to improve the sintering of Sr doped  $\text{LaCrO}_3$  materials. Hitherto, preliminary experimental data on the crystallization of Ca doped  $\text{LaCrO}_3$  under hydrothermal conditions, were recently reported by the present authors [14]. The transformation of an amorphous multicomponent complex gel ( $\text{La}^{3+}$ ,  $\text{Ca}^{2+}$  and  $\text{Cr}^{3+}$ ) into the crystalline orthorhombic  $\text{LaCrO}_3$  phase occurs at low temperature (375 °C) for 1 h. Powders with a peculiar irregular peanut-like shape and small size of 300 nm were obtained by the hydrothermal treatment, and these powders had good sinterability to achieve high relative densities (>96%) by heat treatments carried out at 1400 °C for 5 h in air. Hence, the present work is aimed to determine the feasibility of obtaining single phase  $\text{La}_{1-x}\text{Sr}_x\text{CrO}_3$  powders by ordinary hydrothermal treatments. Additional experiments were conducted to investigate the sintering of the fine powders by heat treatments in air. Furthermore, the differences on the microstructure of the specimens sintered under these conditions are discussed on the basis of the size and morphology of the raw powders. The electrical conductivity of the sintered pellets was measured only on the specimens exhibiting relative densities above of 95%.

## 2. Experimental

### 2.1. Hydrothermal synthesis

Precursor lanthanum chromite gel was prepared by the alkaline coprecipitation method reported elsewhere [15]. Reagent grade chemicals of  $\text{LaCl}_3 \cdot 7\text{H}_2\text{O}$  (99.999%),  $\text{Cr}(\text{NO}_3)_3 \cdot 9\text{H}_2\text{O}$  (99%),  $\text{SrCl}_2 \cdot 6\text{H}_2\text{O}$  (99.995%) and  $\text{NaOH}$  (99.998%) (Aldrich Chemical Company, Inc.) were used. Aqueous solutions with a concentration 0.05 M of  $\text{LaCl}_3$ ,  $\text{Cr}(\text{NO}_3)_3$  and  $\text{SrCl}_2$  were prepared with deionized water, while a solution of  $\text{NaOH}$  with a concentration of 0.5 M was employed as coprecipitation media. In a typical procedure, 500  $\text{cm}^3$  of the chromium solution was mixed with 475  $\text{cm}^3$  of  $\text{NaOH}$  solution to get an opaque. The vigorous stirring of the solution resulted in the dissolution of the preliminary precipitated gel of  $\text{Cr}(\text{OH})_3$ , which occurred at a pH value of 12. Finally, the coprecipitation of the complex gel was carried out by pouring the mixture of the La and Sr solution (500  $\text{cm}^3$ ) to the solution containing  $\text{Cr}^{3+}$  ions. The solutions were mixed in two different volumetric ratios, La:Sr:Cr, 0.9:0.1:1 and 0.8:0.2:1, which matches the compositional stoichiometry of the solid solutions,  $\text{La}_{0.9}\text{Sr}_{0.1}\text{CrO}_3$  and  $\text{La}_{0.8}\text{Sr}_{0.2}\text{CrO}_3$ , respectively. The coprecipitated gel was centrifuged, and a volume of 20  $\text{cm}^3$  of gel was then poured into a Hastelloy C-lined microautoclave (40  $\text{cm}^3$  capacity). The vessel was heated at a constant rate of 20°/min up to various temperatures (400–450 °C) for a reaction interval between 0.5 and 2 h. After the treatments, the precipitates were well washed with distilled water, and then dried in an oven at 100 °C overnight.

### 2.2. Sintering

The powders (0.5 g) were placed in a tungsten carbide die (10 mm diameter) and pressed by hand, the formed pellets were then cold isostatically pressed at two different loads of 100 and 200 MPa for 5 min. The green compacts were heated at a constant heating rate of 10°/min up to the desired temperature. The sintering was conducted in air at temperatures of 1400 and 1500 °C for several reaction intervals ranging from 1 to 20 h.

### 2.3. Characterization

Powder X-ray diffraction analyses were carried out to determine the crystalline phases and the lattice parameter constants of the synthesized powder. Measurements were made by an X-ray diffractometer (Rigaku Rotaflex) with graphite-monochromatized  $\text{Cu K}\alpha$  radiation ( $\lambda = 1.54056 \text{ \AA}$ ) at 40 kV and 100 mA. Diffraction patterns were taken from 10 to 70° at a scanning speed of 4°/min. The lattice parameters were calculated by the least square method from the diffraction peaks collected in the  $2\theta$  range from 20 to 60° at a scanning speed of 0.4°/min and step sampling interval of 0.006°, using Si as an internal standard. The theoretical densities of the hydrothermally synthesized powders were calculated from

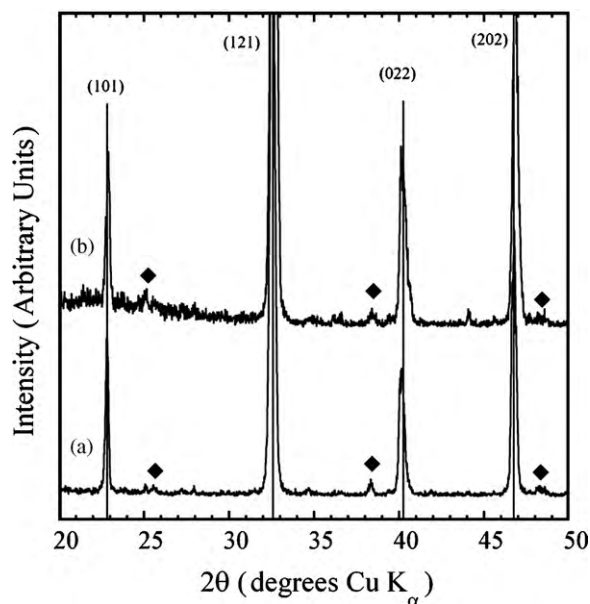


**Fig. 1.** X-ray diffraction patterns of (a)  $\text{La}_{0.9}\text{Sr}_{0.1}\text{CrO}_3$  and (b)  $\text{La}_{0.8}\text{Sr}_{0.2}\text{CrO}_3$  powders obtained under hydrothermal conditions for 1 h at 400 and 425 °C, respectively. Solid line: main diffraction pattern lines and (◆) minor intensity lines of  $\text{LaCrO}_3$  with orthorhombic structure.

the lattice parameters data. Moreover, morphological aspects of the powders were examined by scanning electron microscopy (SEM, Philips XL30 ESEM) equipped with an energy dispersive X-ray (EDX) analyzer. In addition, the particle size was measured by transmission electron microscopy (TEM, Hitachi H-800).

The sintered specimens were polished to mirror like surface, followed by thermal etching at 1275 °C for 3 h in order to reveal the grain boundary, and to conduct the grain size measurements. The relative density of the sintered specimens was determined by Archimedes's principle using a helium pycnometer (Multipycnometer Quantachrome). Each relative density value corresponds to an average of five measurements, which were carried out at a constant helium pressure of 0.117 MPa.

## 3. Results and discussion

### 3.1. Hydrothermal synthesis of $\text{La}_{0.9}\text{Sr}_{0.1}\text{CrO}_3$ and $\text{La}_{0.8}\text{Sr}_{0.2}\text{CrO}_3$ powders

The lowest temperatures required to achieve the crystallization of  $\text{LaCrO}_3$  single phase were determined by varying the reaction temperature in the range between 400 and 425 °C. Fig. 1 shows typical X-ray diffraction patterns of the  $\text{La}_{0.9}\text{Sr}_{0.1}\text{CrO}_3$  and  $\text{La}_{0.8}\text{Sr}_{0.2}\text{CrO}_3$  powders prepared at 400 and 425 °C, respectively. The results show the formation of the orthorhombic  $\text{LaCrO}_3$  single phase (JCPDS 33-701) without any reaction by-products. Furthermore, these results also depict that the crystallization temperature under hydrothermal conditions, depends markedly on the amount of  $\text{Sr}^{2+}$  incorporated into the A-site of the perovskite structure. One point that deserves emphasis is that below these temperatures (400 or 425 °C), the crystallization of the orthorhombic perovskite phase did not proceed. These results are similar to those previously reported for the crystallization of  $\text{La}_{1-x}\text{Ca}_x\text{CrO}_3$ , prepared under similar hydrothermal conditions [14]. The X-ray diffraction patterns of the lanthanum chromite solid solutions,  $\text{La}_{0.9}\text{Sr}_{0.1}\text{CrO}_3$  and  $\text{La}_{0.8}\text{Sr}_{0.2}\text{CrO}_3$ , showed a gradual shifting to high angle. This peak displacement might be associated with the formation of the  $\text{La}_{1-x}\text{Sr}_x\text{CrO}_3$  solid solutions, due to the incorporation of  $\text{Sr}^{2+}$  with a small ionic radius (1.12 Å) in comparison with  $\text{La}^{3+}$  (1.06 Å). Indeed, the decrease in the lattice parameters of Sr doped powders (Table 1) from those of the pure  $\text{LaCrO}_3$  powder crystallized under hydrothermal conditions is in agreement with the inference proposed above. However, the peak displacement is less than that

**Table 1**

Theoretical density calculated from lattice parameters obtained by powder X-ray diffraction patterns. La, Sr and Cr contents (mol%) were estimated from the EDX spectra and the nominal La:Sr:Cr.

Composition	EDX analyses			La:Ca:Cr	Lattice parameters			Cell volume (Å <sup>3</sup> )	Theoretical density (g/cm <sup>3</sup> )
	La (at.%)	Sr (at.%)	Cr (at.%)		a (Å)	b (Å)	c (Å)		
La <sub>0.9</sub> Sr <sub>0.1</sub> CrO <sub>3</sub>	45.1(5)	4.98(5)	49.92(5)	0.9:0.1:1.0	5.4667(9)	5.5043(9)	7.7593(9)	233.48	6.6494
La <sub>0.8</sub> Sr <sub>0.2</sub> CrO <sub>3</sub>	40.05(5)	10.02(5)	49.93(5)	0.8:0.2:1.0	5.4397(9)	5.4986(9)	7.7621(9)	232.17	6.5402

of the lanthanum chromite doped with calcium [14], because of the small difference between the ionic radius of Sr<sup>2+</sup> and La<sup>3+</sup> which is 0.057 Å.

SEM images of powders corresponding to the solid solutions of La<sub>0.9</sub>Sr<sub>0.1</sub>CrO<sub>3</sub> and La<sub>0.8</sub>Sr<sub>0.2</sub>CrO<sub>3</sub> are shown in Fig. 2; these powders were obtained after hydrothermal treatments conducted at 400 and 425 °C for 1 h, respectively. In general, the SEM micrographs reveal the formation of particles with submicron size and irregular morphology which resembles a peanut-like shape. Furthermore, due to these morphological aspects the particles showed a marked agglomeration.

Additional aspects of the particles were revealed by TEM micrographs on La<sub>0.9</sub>Sr<sub>0.1</sub>CrO<sub>3</sub> and La<sub>0.8</sub>Sr<sub>0.2</sub>CrO<sub>3</sub> particles (Fig. 3) hydrothermally synthesized for 1 h at 400 and 425 °C, respectively. At reaction intervals over 1 h, it was found that the particles exhibit a marked tendency for particle bonding. These are clear evidences that indicate the particles were partially dissolved in the fluid at an intermediate reaction stage (>1 h) of the hydrothermal treatment. The TEM observations showed that the peanut-like shaped La<sub>1-x</sub>Sr<sub>x</sub>CrO<sub>3</sub> particles prepared under hydrothermal conditions have an average particle size of 300 nm, the particle size was estimated from the SEM images of 50 particles. Based on the preliminary characterization results, it is expected that these fine powders should exhibit a better sinterability even in oxidizing atmospheres.

In ordinary hydrothermal treatments, the recrystallization and growth process of a stable oxide compound is achieved by a mechanism of dissolution-crystallization [16–18]. In this case, the starting materials dissolved in a solvent and the compound is

formed by homogenous nucleation followed by a hydrothermal particle growth. The resulting particles have a specific morphology depending on their crystalline structural habit and particle growing conditions. One particular example related with the preparation of LaCrO<sub>3</sub> powders with cubic morphology was recently reported by Zheng et al. [19] These authors found that a slurry constituted by a stoichiometric mixture of La<sub>2</sub>O<sub>3</sub>·xH<sub>2</sub>O:CrCl<sub>3</sub>:KOH (1:1–1.1:10–80) crystallized to perovskite LaCrO<sub>3</sub> particles with a cubic morphology and a narrow size distribution between 1 and 3 μm under hydrothermal conditions, at temperatures between 240 and 260 °C for 1 week with concentrated alkaline KOH solution (8–10 M). The LaCrO<sub>3</sub> particle growth was further accelerated by increasing the temperature. Furthermore, similar results were found for the synthesis of the perovskite La<sub>0.5</sub>Sr<sub>0.5</sub>MnO<sub>3</sub> compound under subcritical hydrothermal conditions. La<sub>0.5</sub>Sr<sub>0.5</sub>MnO<sub>3</sub> particles exhibiting a cubic shape habit were preferentially formed in a concentrated alkaline solution of KOH, which contained the stoichiometric amount of the compounds KMnO<sub>4</sub>, MnCl<sub>2</sub>, SrSO<sub>4</sub> and La(NO<sub>3</sub>)<sub>3</sub>. The cubic La<sub>0.5</sub>Sr<sub>0.5</sub>MnO<sub>3</sub> particles with a size approximately of 1 μm, were produced at 240 °C for 24 h [20].

However, the synthesis of La<sub>1-x</sub>Sr<sub>x</sub>CrO<sub>3</sub> powders in this study cannot be explained by the mechanism described above. In our case, the dissolution-crystallization mechanism which promotes the homogeneous nucleation and formation of dispersed particles was further limited during the heating and early stages of the reaction, because the hydrothermal solvent was not poured into

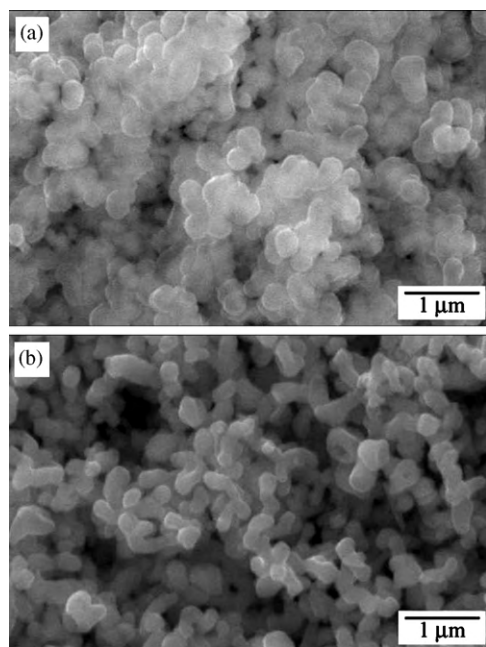


**Fig. 2.** SEM micrograph of Sr doped LaCrO<sub>3</sub> powders obtained under hydrothermal conditions for 1 h at several temperatures: (a) La<sub>0.9</sub>Sr<sub>0.1</sub>CrO<sub>3</sub> at 400 °C and (b) La<sub>0.8</sub>Sr<sub>0.2</sub>CrO<sub>3</sub> at 425 °C.

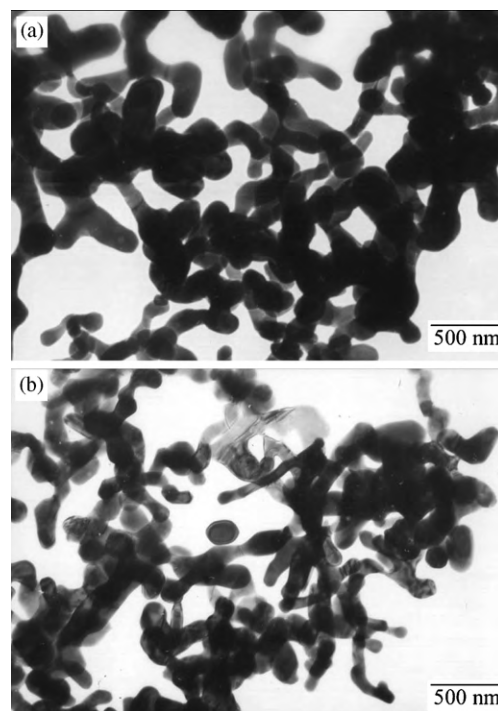


**Fig. 3.** TEM micrograph of solid solutions of lanthanum chromite powders obtained under hydrothermal conditions for a time interval of 1 h: (a) La<sub>0.9</sub>Sr<sub>0.1</sub>CrO<sub>3</sub> at 400 °C and (b) La<sub>0.8</sub>Sr<sub>0.2</sub>CrO<sub>3</sub> at 425 °C.

the vessel together with the precursor gel. The hydrothermal solvent chemically reacts with the solid species incorporated in the vessel; this produces the dissolution of any solid and simultaneously the ionic saturation of the solvent proceeds, which results in the spontaneous precipitation as was reported for the  $\text{LaCrO}_3$  and  $\text{La}_{0.5}\text{Sr}_{0.5}\text{MnO}_3$  powders. In contrast, based on preliminary observations conducted even during the heating stage of treatment, these confirmed that the hydrothermal synthesis studied involves a preliminary reaction stage which is related with the decomposition of the precursor gel, which proceeds by a dehydration process. The gel dehydration proceeds at temperatures above  $300^\circ\text{C}$  and simultaneously leads to the formation of hydrothermal solvent inside the reaction vessel. It was confirmed that the autogenously formed liquid was a low concentrated alkaline solution, because the pH of the remaining solution after the hydrothermal treatment was 7.42. Hence, the dissolution of the starting materials must be limited in such a diluted alkaline solution. We expect that the nucleation of the oxide particles proceeds preferentially at the surface of the remaining gel during the dehydration process, because the crystallization by the process employed in this study proceeded at higher temperatures ( $300\text{--}450^\circ\text{C}$ ) [18,21] than those determined for  $\text{LaCrO}_3$  and  $\text{La}_{0.5}\text{Sr}_{0.5}\text{MnO}_3$  particles under concentrated alkaline hydrothermal conditions,  $240$  and  $260^\circ\text{C}$ , respectively.

Additionally, we surmise that two main factors promoted the formation of the peanut-like shaped particles obtained in this study; the first is related with the nucleation and growth process which proceeded very fast for reaction intervals of 0.5 up to 2 h at the selected temperatures ( $400\text{--}450^\circ\text{C}$ ) and limited the growth of  $\text{La}_{1-x}\text{Sr}_x\text{CrO}_3$  particles. The second one is associated with the concentration of the alkaline solvent media; the alkaline fluid autogenously formed during the hydrothermal treatment is not capable of achieving the conditions which lead the crystallization of particles with cubic habit [19,20]. However, the  $\text{La}_{1-x}\text{Sr}_x\text{CrO}_3$  particles were partially dissolved in the solvent media at high temperature ( $400\text{--}450^\circ\text{C}$ ), resulting in a slight particle joining by developing neck on their surfaces in contact as shown in Fig. 3 for both  $\text{La}_{0.9}\text{Sr}_{0.1}\text{CrO}_3$  and  $\text{La}_{0.8}\text{Sr}_{0.2}\text{CrO}_3$  powders. This local recrystallization of the solute is mainly promoted inside the reaction vessel, due to the fact that no fluid convection occurred during the hydrothermal treatment, because the treatments were conducted under static conditions at constant temperature, therefore, mass transfer due to convection was further limited [22].

### 3.2. Sintering of hydrothermally derived $\text{La}_{0.9}\text{Sr}_{0.1}\text{CrO}_3$ and $\text{La}_{0.8}\text{Sr}_{0.2}\text{CrO}_3$ powders

The relative density of the pellets after sintering was calculated based on the apparent density measured by helium pycnometry against the theoretical density determined from the lattice parameters of each solid solution. Thus, the variation of the relative density for  $\text{La}_{0.9}\text{Sr}_{0.1}\text{CrO}_3$  and  $\text{La}_{0.8}\text{Sr}_{0.2}\text{CrO}_3$  samples sintered in air for several reaction times at  $1500^\circ\text{C}$ , is shown in Fig. 4. In general, the relative density of the  $\text{La}_{0.9}\text{Sr}_{0.1}\text{CrO}_3$  and  $\text{La}_{0.8}\text{Sr}_{0.2}\text{CrO}_3$  samples increases gradually with the increase of the reaction time. However, beyond 10 h, the relative density of the pellets was almost constant. The maximum density determined on the  $\text{La}_{0.8}\text{Sr}_{0.2}\text{CrO}_3$  specimen was approximately 97.2%, while the highest relative density achieved on the samples of  $\text{La}_{0.9}\text{Sr}_{0.1}\text{CrO}_3$  was 86.7%. The maximum values of the densities obtained for the hydrothermally synthesized  $\text{La}_{0.8}\text{Sr}_{0.2}\text{CrO}_3$  powders are similar to those reported for Sr doped  $\text{LaCrO}_3$  powders containing 20 mol% Sr prepared by the Pechini method, the uniaxially pressed powders at 100 MPa [12] and 200 MPa [10] reached relative densities values of 95% and 96.0%, when the pellets were sintered at temperatures of  $1600$  and  $1740^\circ\text{C}$  in a mixture of  $\text{N}_2$ ,  $\text{CO}_2$  and  $\text{H}_2$  atmosphere, respectively. Furthermore, a relative density values above 95% were

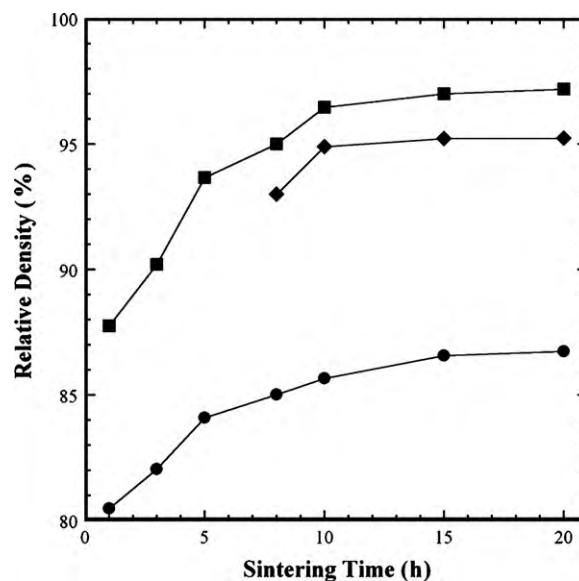


Fig. 4. Variation of the relative density of (a)  $\text{La}_{0.9}\text{Sr}_{0.1}\text{CrO}_3$  (●) and  $\text{La}_{0.8}\text{Sr}_{0.2}\text{CrO}_3$  (■) pellets cold isostatically pressed at 200 MPa, and those corresponding to the  $\text{La}_{0.8}\text{Sr}_{0.2}\text{CrO}_3$  pellets (◆) cold isostatically pressed at 100 MPa. The sintering of the hydrothermally synthesized  $\text{La}_{0.9}\text{Sr}_{0.1}\text{CrO}_3$  and  $\text{La}_{0.8}\text{Sr}_{0.2}\text{CrO}_3$  pellets produced was conducted at  $1500^\circ\text{C}$  in air atmosphere for various reaction intervals.

successfully achieved when the hydrothermally  $\text{La}_{0.8}\text{Sr}_{0.2}\text{CrO}_3$  synthesized powders were cold isostatic pressed even at a lower load of 100 MPa, these values were achieved at a sintering interval above 8 h at  $1500^\circ\text{C}$  in air (marker ◆ in Fig. 4). These results demonstrate that the hydrothermally synthesized peanut-like shaped  $\text{La}_{0.8}\text{Sr}_{0.2}\text{CrO}_3$  particles exhibit a better sinterability behavior in air, in comparison with the same composition of particles prepared by soft chemistry methods [10,12].

Moreover, other point that deserves emphasis is related with the chemical stability of the  $\text{La}_{0.9}\text{Sr}_{0.1}\text{CrO}_3$  and  $\text{La}_{0.8}\text{Sr}_{0.2}\text{CrO}_3$  powders. This factor can be affected by the thermal stability of the doped lanthanum chromite material, because the chromium evaporation is difficult to avoid during the sintering stage [23]. This was reported to occur on the powders prepared by Pechini's method with similar compositional amount of doping to those used in the present work [10,12]. This is a relevant phenomenon to avoid in the related chromium based lanthanum perovskites, therefore, efforts in order to reduce this process involved the incorporation of other elements such as Mn [23]. However, the present results demonstrated that the hydrothermally derived  $\text{La}_{1-x}\text{Sr}_x\text{CrO}_3$  powders did not undergo a significant loss of  $\text{Cr}^{3+}$  during the sintering stage in either cases studied. This behavior was revealed even for the samples treated for long sintering intervals over 15 h in air atmosphere. This inference is supported by compositional analyses conducted by EDX for sintered pellets of  $\text{La}_{0.9}\text{Sr}_{0.1}\text{CrO}_3$  and  $\text{La}_{0.8}\text{Sr}_{0.2}\text{CrO}_3$  at  $1500^\circ\text{C}$  for 20 h. The analyses yielded the atomic ratios of La: Sr: Cr = 45.09(5):4.97(5):49.94(5) and 40.04(5):10.05(5):49.90(5). These values are nearly similar with the nominal stoichiometric compositions for the solid solutions of  $\text{La}_{0.9}\text{Sr}_{0.1}\text{CrO}_3$  and  $\text{La}_{0.8}\text{Sr}_{0.2}\text{CrO}_3$  (Table 1), respectively.

### 3.3. Microstructure of sintered $\text{La}_{0.9}\text{Sr}_{0.1}\text{CrO}_3$ and $\text{La}_{0.8}\text{Sr}_{0.2}\text{CrO}_3$ pellets

The microstructure of the sintered pellets was examined after thermal etching using a scanning electron microscope (SEM). Fig. 5 shows the typical aspects of the microstructure for  $\text{La}_{0.9}\text{Sr}_{0.1}\text{CrO}_3$  pellets sintered at  $1500^\circ\text{C}$  in air for intervals of 8 and 20 h. In general, the microstructure of both samples sintered for short and long

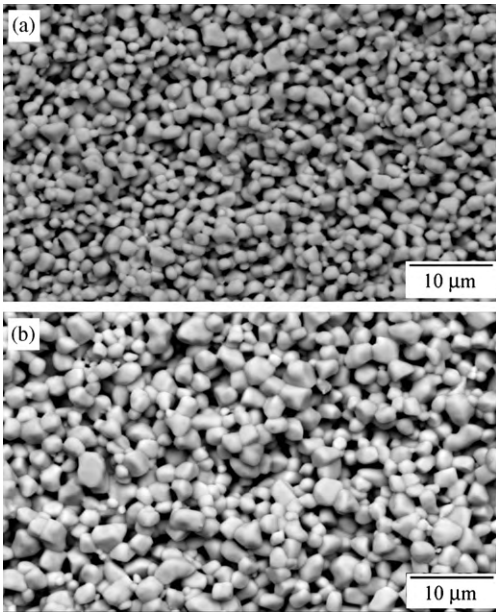


**Fig. 5.** SEM micrograph of samples  $\text{La}_{0.9}\text{Sr}_{0.1}\text{CrO}_3$  sintered at  $1500^\circ\text{C}$  for (a) 8 h, and (b) 20 h in air.

intervals shows the presence of a high amount of residual porosity. At 8 h, the microstructure of the pellet consists of very fine grains with an average size of  $1\ \mu\text{m}$ , and also a few neck bonding points between the particles are clearly observed (Fig. 5a). A slight grain growth of some large particles ( $\sim 2.5\ \mu\text{m}$ ) is promoted by increasing the sintering interval up to 20 h (Fig. 5b). These observations are in accordance with the low relative densities of the  $\text{La}_{0.9}\text{Sr}_{0.1}\text{CrO}_3$  pellets, as shown in Fig. 4. The limited densification achieved on sintered at  $1500^\circ\text{C}$  might be explained in terms of the small amount of  $\text{Sr}^{2+}$  incorporated into the structure of the nominal  $\text{La}_{0.9}\text{Sr}_{0.1}\text{CrO}_3$  solid solution, because as it commonly accepted, the sintering of Sr doped  $\text{LaCrO}_3$  powders is normally promoted by the formation of a transitory liquid phase, corresponding to  $\text{SrCrO}_4$  liquid that forms at  $1275^\circ\text{C}$  [24]. Since that liquid is normally located at the grain boundaries, powder densification is affected because the markedly limited mass transfer across the growing grain boundaries [25]. In summary, the lim-

ited amount and heterogeneous distribution of the  $\text{SrCrO}_4$  liquid within the grains boundaries result in an insufficiency to achieve the densification of the  $\text{La}_{0.9}\text{Sr}_{0.1}\text{CrO}_3$  peanut-like shaped particles even at high temperature ( $1500^\circ\text{C}$ ). This inference is supported by the fact that the  $\text{LaCrO}_3$  samples doped with 20 mol% Sr exhibited more dense microstructures formed by equiaxed grains, but some residual porosity was also observed (Fig. 6).

On the other hand, microstructural studies conducted on doped lanthanum chromite powders densified with different sintering aids, namely strontium vanadate [5], demonstrated that the typical microstructure of the fully densified specimens is constituted by equiaxial grains. Thus, the microstructure of the  $\text{La}_{0.85}\text{Sr}_{0.15}\text{CrO}_3$  powder mixed with 10 wt% of  $\text{Sr}_3(\text{VO}_4)_2$  sintered at  $1550^\circ\text{C}$  for 2 h, is very similar to that of the  $\text{La}_{0.8}\text{Sr}_{0.2}\text{CrO}_3$  pellets obtained at  $1500^\circ\text{C}$  for 15 h, because this sample resembles a similar microstructure of the  $\text{La}_{0.85}\text{Sr}_{0.15}\text{CrO}_3$  produced by adding a sintering aid agent. In contrast, the  $\text{La}_{0.8}\text{Sr}_{0.2}\text{CrO}_3$  pellets sintered between 8 and 15 h exhibited a marked abnormal grain growth, resulting in a heterogeneous equiaxial grain size microstructure. Hitherto, it is well known that the abnormal grain growth is mainly achieved by several factors, namely secondary phases, impurities, pores or inclusions, which might further affect the mobility of the grain boundary [24,26]. Furthermore, the presence of a liquid phase at the grain boundaries could also affect the grain coarsening, which might occur at low speed in those areas where an incipient amount of liquid is produced, which achieves the discontinuous grain growth during the sintering stage [26]. However, based on the microstructural observations (Fig. 6) conducted on both sintered pellets and raw hydrothermally derived powders, we suggest an additional factor which promotes the discontinuous grain growth, that is the morphology of the raw powder. Because some of the raw  $\text{La}_{0.9}\text{Sr}_{0.2}\text{CrO}_3$  particles were already bonded and agglomerated, it is expected that the sintering proceeds fast in these particles, in comparison with the sintering behavior of the monodispersed small particles even at intermediate sintering intervals. This factor coupled with the liquid assisted sintering process might result in the abnormal grain growth observed. Hence, we suggest that when the porosity was reduced in the pellet and the transitory liquid was homogeneously distributed along the grain boundaries at sintering intervals of 10 h, this resulted in the achievement of the Ostwald Ripening's grain coarsening process. Thus, the microstructure of the pellets sintered for more than 15 h became more homogeneous in grain size ( $\sim 5\ \mu\text{m}$ ) and shape.

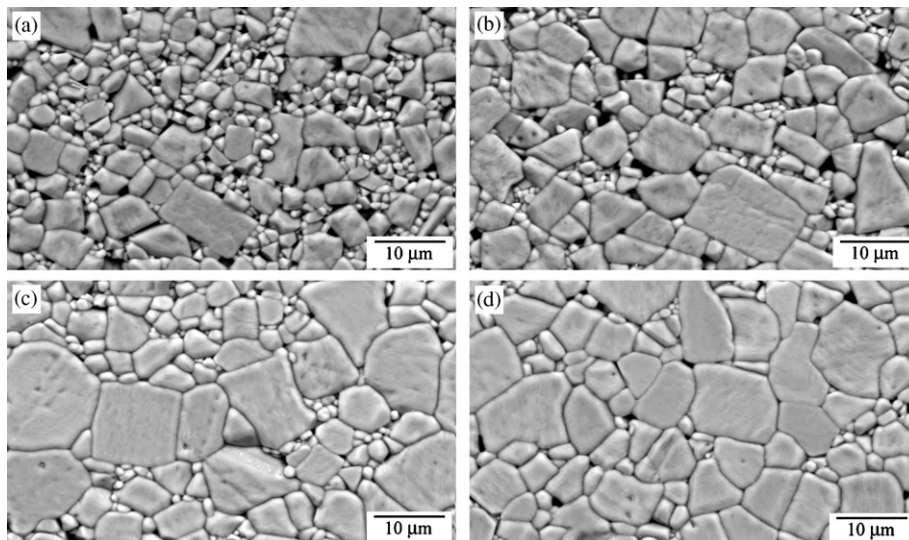


**Fig. 6.** SEM micrograph of samples  $\text{La}_{0.8}\text{Sr}_{0.2}\text{CrO}_3$  sintered at  $1500^\circ\text{C}$  for (a) 8 h, (b) 10 h, (c) 15 h, and (d) 20 h in air.

### 3.4. Electrical conductivity of the $\text{La}_{0.8}\text{Sr}_{0.2}\text{CrO}_3$ sintered pellet

In addition, the electrical conductivity of highly dense  $\text{La}_{0.8}\text{Sr}_{0.2}\text{CrO}_3$  cylindrical pellets (diameter 5 mm and length 20 mm) sintered at 1500 °C for 20 h with a relative density of 97.2%, was measured by the four-probe method in the temperature range from 50 to 1000 °C in air atmosphere using platinum wire as electrodes. It was found that the sintered  $\text{La}_{0.8}\text{Sr}_{0.2}\text{CrO}_3$  specimens had an electric conductivity value of  $1477.3 \text{ S m}^{-1}$ , with an activation energy of 0.13 eV. These electrical properties are within those measured for a wide compositional range of alkaline earth doped  $\text{LaCrO}_3$  previously reported [27,28]. Hence, we surmise that hydrothermally prepared  $\text{La}_{0.8}\text{Sr}_{0.2}\text{CrO}_3$  powders at very low temperature (425 °C) by a single step seem to be attractive for industrial application in the manufacturing of SOFCs separator material, because they can reach high relative density values of ~97.0% at 1500 °C for intervals as short as 15 h and the sintering compact exhibits an optimum electrical conductivity.

### 4. Conclusions

Fine powders of strontium doped lanthanum chromite,  $\text{La}_{0.9}\text{Sr}_{0.1}\text{CrO}_3$  and  $\text{La}_{0.8}\text{Sr}_{0.2}\text{CrO}_3$ , were successfully obtained under hydrothermal conditions at low temperatures (400 and 425 °C) for 1 h. The hydrothermally derived  $\text{La}_{0.9}\text{Sr}_{0.1}\text{CrO}_3$  and  $\text{La}_{0.8}\text{Sr}_{0.2}\text{CrO}_3$  particles having a peculiar morphology, resembling peanut-like shaped particles with an average size of 300 nm were preferentially crystallized. Although, the two powders corresponding to  $\text{La}_{0.9}\text{Sr}_{0.1}\text{CrO}_3$  and  $\text{La}_{0.8}\text{Sr}_{0.2}\text{CrO}_3$  solid solutions did not sinter at 1400 °C, however,  $\text{Cr}^{3+}$  evaporation did not take place on the powders that underwent densification at 1500 °C, even those specimens treated at sintering intervals above 15 h. Furthermore, a poor sinterability in air atmosphere was determined for the  $\text{La}_{0.9}\text{Sr}_{0.1}\text{CrO}_3$  powder prepared under hydrothermal conditions, it might be due to the amount of transient liquid, which was not sufficient to achieve mass transfer as well as powder densification. In contrast, highly dense  $\text{La}_{0.8}\text{Sr}_{0.2}\text{CrO}_3$  pellets were obtained by firing at 1500 °C for 20 h. The maximum densification obtained in the pellets of  $\text{La}_{0.8}\text{Sr}_{0.2}\text{CrO}_3$  was 97% of the theoretical density; and the equiaxed grain size was approximately 5  $\mu\text{m}$ . In addition, a markedly abnormal grain growth was observed to occur mainly in the 20 mol% Sr doped  $\text{LaCrO}_3$  powders; this phenomenon is associated to the transient liquid formation and the heterogeneity on the raw powder particle size and morphology. Furthermore, the electrical conductivity of the cylindrical  $\text{La}_{0.8}\text{Sr}_{0.2}\text{CrO}_3$  pellet sintered at 1500 °C for 20 h was measured in air. The value determined was  $1477.3 \text{ S m}^{-1}$ , while the activation energy was 0.13 eV.

### Acknowledgements

One of the authors, J.C.R.A., is indebted to CONACYT, Mexico, for financial support in the form of a Sabbatical research grant, additional support was received through the research fund (Project CONACYT CB 2004-P47259-Y); the authors also acknowledge the support of CINESTAV (Mexico) in order to conduct the present research. Many thanks are offered to Eng. Felipe de Jesús Márquez Torres of CINESTAV–Saltillo, who helped in the preparation of samples for SEM observations.

### References

- [1] I. Yasuda, M. Hishinuma, *Solid State Ionics* 80 (1995) 141–150.
- [2] A. Kajimura, H. Sasaki, S. Otsoshi, M. Suzuki, M. Ippommatsu, T. Kawai, S. Kawai, *Solid State Ionics* 76 (1995) 41–46.
- [3] D.H. Peck, M. Miller, K. Hilpert, *Solid State Ionics* 143 (2001) 401–412.
- [4] P. Vernoux, E. Djurado, M. Guillodo, *J. Am. Ceram. Soc.* 84 (2001) 2289–2295.
- [5] S.P. Simmer, J.S. Hardy, J.W. Stevenson, T.R. Armstrong, *Solid State Ionics* 128 (2000) 53–63.
- [6] T. Takeuchi, Y. Takeda, R. Funahashi, T. Aihara, M. Tabuchi, H. Kageyama, *J. Electrochem. Soc.* 147 (2000) 3979–3982.
- [7] N.M. Sammes, C.E. Hatchwell, *Mater. Lett.* 32 (1997) 339–345.
- [8] K. Deshpande, A. Mukasyan, A. Varma, *J. Am. Ceram. Soc.* 86 (2003) 1149–1154.
- [9] J. Owenstone, C.B. Ponton, *J. Mater. Sci. Lett.* 35 (2000) 4115–4119.
- [10] L. Group, H.U. Anderson, *J. Am. Ceram. Soc.* 59 (1976) 449–450.
- [11] M. Mori, N.M. Sammes, *Solid State Ionics* 146 (2002) 301–312.
- [12] E. Suda, B. Pacaud, T. Seguelong, Y. Takeda, *Solid State Ionics* 151 (2002) 335–341.
- [13] L.W. Tai, P.A. Lessing, *J. Am. Ceram. Soc.* 74 (1991) 155–160.
- [14] L.P. Rivas-Vázquez, J.C. Rendón-Angeles, J.L. Rodríguez-Galicia, K.J. Zhu, K. Yanagisawa, *Solid State Ionics* 172 (2004) 389–392.
- [15] M. Inagaki, O. Yamamoto, M. Hirohara, *Ceram. Soc. Jpn.* 98 (1990) 675–678.
- [16] M. Yoshimura, S.T. Song, S. Somiya, *Yogyo-Kyokai-Shi* 90 (1982) 91–95.
- [17] Z. Chen, E. Shi, W. Li, Y. Zheng, N. Wu, W. Zhong, *J. Am. Ceram. Soc.* 85 (2002) 2949–2955.
- [18] M.M. Lencka, R.E. Riman, *Chem. Mater.* 7 (1995) 18–25.
- [19] W. Zheng, W. Pang, G. Meng, D. Peng, *J. Mater. Chem.* 9 (1999) 2833–2836.
- [20] J. Spooren, A. Rumpelcker, F. Millange, R.I. Walton, *Chem. Mater.* 15 (2003) 1401–1403.
- [21] L.P. Rivas-Vázquez, J.C. Rendón-Angeles, J.L. Rodríguez-Galicia, C.A. Gutierrez-Chavarria, K.J. Zhu, K. Yanagisawa, *J. Eur. Ceram. Soc.* 26 (2006) 81–88.
- [22] K. Byrappa, M. Yoshimura, *Handbook of Hydrothermal Technology*, Noyes Publications/William Andrew Publishing, Norwich, NY, USA, 2001, pp. 754–772 (Chapter 10).
- [23] B.P. McCarthy, L.R. Pederson, R.E. Williford, D.Z. Xiao, *J. Am. Ceram. Soc.* 92 (2009) 1672–1678.
- [24] Y.J. Yang, T.L. Wen, H. Tu, D.Q. Wang, J. Yang, *Solid State Ionics* 135 (2000) 475–479.
- [25] M.W. Barsoum, *Sintering and Grain Growth, Fundamentals of Ceramics*, Institute of Physics Publishing Ltd, United Kingdom, 2003, pp. 302–355 (Chapter 10).
- [26] T.W. Sone, J.H. Han, *J. Am. Ceram. Soc.* 84 (2001) 1386–1388.
- [27] N. Sakai, T. Kawada, H. Yokokawa, M. Dokiya, *J. Mater. Sci.* 25 (1990) 4531–4534.
- [28] N. Sakai, H. Yokokawa, T. Horita, K. Yamaji, *Int. J. Appl. Ceram. Technol.* 1 (2004) 23–30.